Mathematical modelling of COVID-19 transmission dynamics with vaccination: A case study in Ethiopia

Sileshi Sintayehu Sharbayta[1] , Henok Desalegn[1] and Tadesse Abdi[1]

[1] *Department of Mathematics, Addis Ababa University, Addis Ababa, Ethiopia*

Correspondence should be addressed to Sileshi Sintayehu Sharbayta ; sileshi.sintayehu@aau.edu.et

Abstract

In this paper, we consider a mathematical model of COVID-19 transmission with vaccination where the total population was subdivided into nine disjoint compartments, namely, Susceptible(S), Vaccinated with the first dose(V_1), Vaccinated with the second dose(V_2), Exposed (E), Asymptomatic infectious (I), Symptomatic infectious (I), Quarantine (Q), Hospitalized (H) and Recovered (R). We computed a reproduction parameter, R_v, using the next generation matrix. Analytical and numerical approach is used to investigate the results. In the analytical study of the model: we showed the local and global stability of disease-free equilibrium, the existence of the endemic equilibrium and its local stability, positivity of the solution, invariant region of the solution, transcritical bifurcation of equilibrium and conducted sensitivity analysis of the model. From these analysis, we found that the disease-free equilibrium is globally asymptotically stable for $R_v < 1$ and unstable for $R_v > 1$. A locally stable endemic equilibrium exists for $R_v > 1$, which shows persistence of the disease if the reproduction parameter is greater than unity. The model is fitted to cumulative daily infected cases and vaccinated individuals data of Ethiopia from May $01, 2021$ to January $31, 2022$. The unknown parameters are estimated using the least square method with built-in MATLAB function 'lsqcurvefit'. Finally, we performed different simulations using MATLAB and predicted the vaccine dose that will be administered at the end of two years. From the simulation results, we found that it is important to reduce the transmission rate, infectivity factor of asymptomatic cases and increase the vaccination rate, quarantine rate to control the disease transmission. Predictions show that the vaccination rate has to be increased from the current rate to achieve a reasonable vaccination coverage in the next two years.

Keywords: COVID-19, Vaccination, Control reproduction number, Sensitivity analysis, Endemic equilibrium, Parameter estimation.

1. Introduction

Corona Virus (COVID-19) is an infectious disease caused by a novel corona virus which is a respiratory illness that can spread in a population in several different ways. A person can be infected when droplets containing the virus are inhaled or come directly into contact with the eyes, nose, or mouth. The novel corona virus has been spreading worldwide starting from the first identification in December 2019. The world health organization (WHO) declared COVID-19 as a pandemic on march 12, 2020. Starting from the first day of the outbreak to March 9, 2022, more than 446.5 million confirmed cases and more than 6 million confirmed deaths are registered worldwide [25]. The same report shows 469007 confirmed cases and $7,476$ confirmed deaths in the same period of time in Ethiopia.

The world is struggling to control the pandemic by imposing different restrictions based on country-specific strategies. Besides the restrictions, nowadays different countries are delivering vaccines for their people. As of day 7 March 2022 , 10 vaccines were granted for emergency use by WHO [24]. These are Novavax, COVOVAX, Moderna, Pfizer/BioNTech, Janssen (Johnson & Johnson), AstraZeneca, Covishield (Oxford/AstraZeneca formulation), Covaxin, Sinopharm and Sinovac. Country approvals of this vaccine

differ. For example, Pfizer/BioNTech and Oxford/AstraZeneca are approved by 138 countries, Janssen (Johnson & Johnson) is approved by 107, and Moderna is approved by 85 countries worldwide [24]. Until March 07, 2022, about 10.9 billion COVID-19 vaccine doses are administered globally. 63.4% of the world population has received at least one dose of a COVID-19 vaccine and this coverage represents developed counties due to the scarcity of the vaccine in low-income countries. Only 13.6% of people in low-income countries have received at least one dose [21]. Up to 5 March 2022, a total of 26, 178, 996 vaccine doses have been administered in Ethiopia [25].

Studies involving mathematical models of infectious disease are helping the public health authorities by giving insight information through analysis of the dynamics of the disease to make information- based decisions and policy making. These studies are also powerful tools in predicting the future severity of a disease. As far as COVID-19 is concerned, currently there are several such researches which have been conducted and helping the struggle to contain the spread.

Before vaccines are produced, mathematical models for COVID-19 are focused on assessing the impacts of nonpharmaceutical interventions(NPIs) like social distancing, wearing masks, personal hygiene, partial or full lockdown and the like as control strategies. Here we mention some of them: [20, 1, 23, 2, 18, 13, 3]. In [1], the authors studied the population level impact of implementation of behavioural change control measures , the time horizon necessary to reduce the effective contact rate, and the proportion of people under sanitary emergency measures in controlling COVID-19 in Mexico. One of the nonpharmaceutical measures is to wear a face mask, and the quality of the face mask is sometimes debatable, but the study in [13] suggested that broad adaption of even relatively ineffective face masks may significantly reduces the transmission and hospitalization peak and death. For combating COVID-19, the timing of relaxation or termination of nonpharmaceutical measures is essential. From this point of view, the authors in [18] showed the crucial importance of relaxation or termination of strict social distancing measures in determining the future burden of COVID-19 pandemic. In [3], they evaluate and compare the effectiveness of the four types of NPIs of COVID-19, namely: the implementation of mandatory mask, quarantine or isolation, distancing and traffic restriction in 190 countries between 23 January up to 13 April 2020. In their study, they indicated that NPIs can significantly hold the COVID-19 pandemic. Distancing and the implementation of two or more NPIs should be the priority strategies for holding COVID-19.

Currently, vaccines are available as one of and main control strategies. Epidemiological modelers started to incorporate this additional intervention to see the dynamical properties of the disease and sort out some important policy directions to the public health authorities. In this aspect, there are a number of studies, from which [9, 17, 5] can be mentioned. A mathematical model with comorbidity and an optimal control-based framework to decrease COVID-19 was studied in [9]. In this study, the authors found that an optimal strategy with combined measures provide effective protection of the population from COVID-19 with minimum social and economic costs. Even during vaccination nonpharmaceutical interventions are essential and it is shown that relaxing restrictions would cause benefits from vaccination to be lost by increasing case numbers in which vaccination alone is insufficient to contain the outbreak [17]. Another problem in attaining herd immunity in the population is vaccine hesitancy in case vaccination is not mandatory, in which people are the last to decide either to get vaccinated or not. A behavioural modelling approach was used to assess the impact of hesitancy and refusal of vaccine on the dynamics of the COVID-19 [5]. In this paper, the authors showed hesitancy and refusal of vaccination is better contained in case of large information coverage and small memory characteristics.

Some Epidemiological modelling studies of COVID-19 are based on country-specific data. Here we mention few of the studies on COVID-19 modelling in the case of Ethiopia. In [16], the authors considered a mathematical model for the transmission dynamics of COVID-19 by incorporating self-protection behavior changes in the population. Based on the available data of Ethiopia and other countries, they estimated the unknown parameter values using a combination of least squares and Bayesian estimation methods. They

found that the sensitive parameters for the spread of the virus vary from country to country and control of the effective transmission rate (recommended human behavioral change towards self-protective measures) is essential to stop the spread of the virus. A mathematical model of COVID-19 in the case of Ethiopia is also considered in [15], and in the study they found that the spread of COVID-19 can be managed by minimizing the contact rate of infected and increasing the quarantine of exposed individuals. There are also other COVID-19 mathematical modelling for optimal control and assessing the impact of nonpharmaceutical interventions on the dynamics of COVID- 19 which are specific to Ethiopian data [10, 14]. We believe that scientific studies on COVID-19 transmission in the case of Ethiopia are limited and as far as we review there are no mathematical modelling studies considering the current situation (including vaccination). Therefore, in our study we consider a mathematical model of COVID-19 transmission dynamics with vaccination.

The paper is organized as follows: In Section (2), we describe the model and formulation of the differential equation. In Section (3), we carry out the mathematical analysis of the model. Section (4) is devoted to numerical simulation and discussion. In Section (5), we present a prediction of the cumulative vaccine administered with respect to the first dose vaccination rate. Finally, in Section (6), the conclusion is presented.

2. Model description and formulation

In this study, we proposed a model where the total population is divided in to nine compartments. Namely Susceptible, Vaccinated with first dose, vaccinated with second dose, Exposed (Infected but not yet infectious), Asymptomatic infectious, Symptomatic infectious, Quarantine, Hospitalized and Recovered denoted by S, V_1, V_2, E, I_a, I_s, Q, H and R respectively. We assumed that individuals in Q and H class are isolated from the population and therefore they will have a negligible role in transmitting the disease. Therefore, only individuals in I_a and I_s are capable of transmitting the disease. Vaccines available for COVID-19 do not totally prevent infection, therefore individuals in S, V_1 and V_2 class can get infected with the force of infection $h = \beta\frac{\tau I_a + I_s}{N-(Q+H)}$. Such a force of infection is used in most COVID-19 models [15, 10, 4], where β is the transmission rate, τ is the infectivity factor of asymptomatic individuals and N is the total population. Due to the vaccine efficacy, individuals in V_1 and V_2 class are relatively less infected than the fully susceptible ones: they will get infected with reduced vulnerability of $(1-\eta_1)$ and $(1-\eta_2)$ respectively. η_1 measures the efficacy of the first dose vaccine, where as η_2 measures the efficacy after the second dose. Majority of the vaccines approved by WHO are given in two doses with an average recommended time interval between the two doses. We considered this scenario in our model. Susceptible individuals get vaccination (the first dose) at the rate of p_1 and those who got the first dose will get the second dose after an average $1/\alpha$ period of time with the rate p_2. In this study we did not fix a particular vaccine type therefore the value of $1/\alpha$ represents the average time needed to take the second dose. ρ proportion of exposed individuals will move to asymptomatic class and the rest, $(1-\rho)$ proportion will move to the symptomatic class after they finish the incubation period of $\frac{1}{e}$ day, where e is the infection rate. Mostly the symptoms of COVID-19 are similar to other respiratory diseases like common cold and flue, so all symptomatic individuals do not quarantined. Those only tested and confirmed can go to quarantine. Symptomatic individuals get tested and quarantine at the rate of δ. Those quarantined may develop serious illness, in this case they go to hospital at the rate of q_h. Individuals in I_a, I_s, Q and H will recover from the disease at the rate of r_a, r_s, r_q and r_h respectively. Asymptomatic are individuals with less pain and assumed will not die due to the disease. As a consequence, individuals in I_s, Q and H classes die due to the disease at the rate of d (assumed to be equal). People in all compartments will die naturally at the rate of μ and π is the recruitment rate to the susceptible compartment. The total population size at time t is denoted by $N(t)$ where,

$$N(t) = S(t) + V_1(t) + V_2(t) + E(t) + I_a(t) + I_s(t) + Q(t) + H(t) + R(t). \tag{1}$$

The model flow diagram is shown in Figure 1.

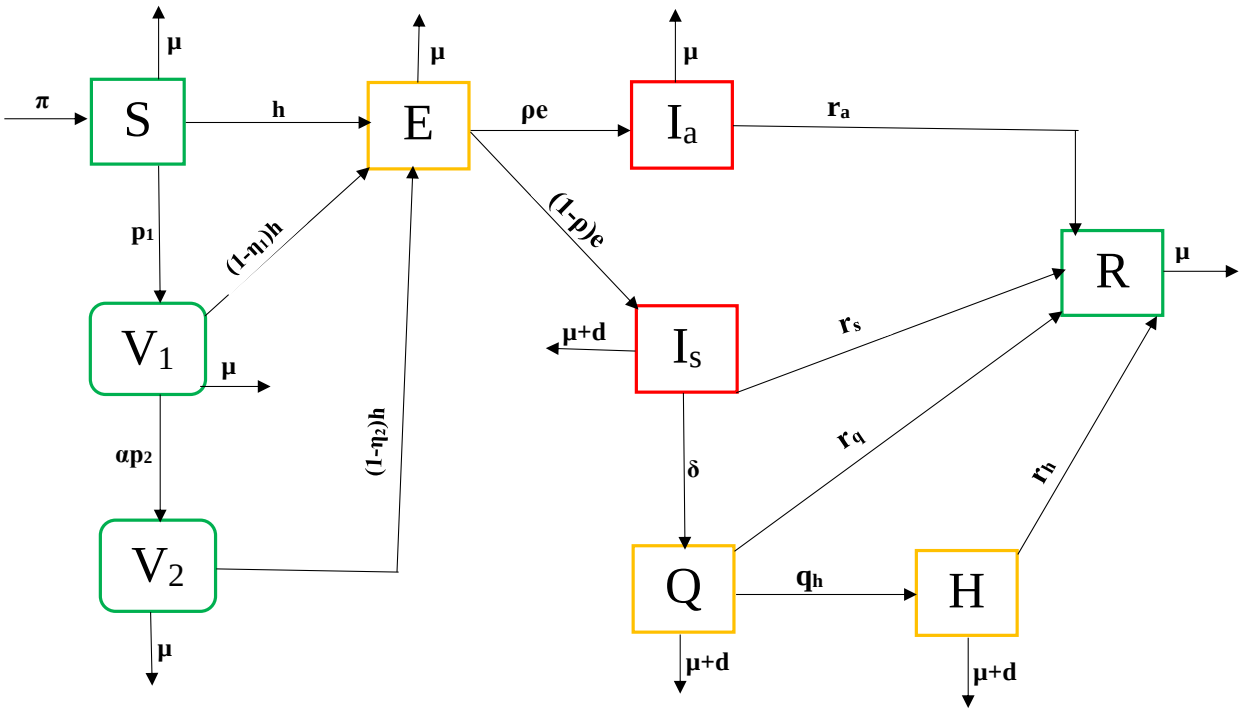

Figure 1: Disease transmission diagram: green compartment indicates non-infected, the red compartment is infected and infectious and the yellow compartment shows infected but assumed to be not infectious(Q and H), on incubation period (H).

From the schematic diagram Figure(1) the following system of differential equation is obtained

$$\begin{cases} \frac{dS}{dt} = \pi - \big(p_1 + \mu + h\big)S \\ \frac{dV_1}{dt} = p_1 S - \big(\alpha p_2 + \mu + (1-\eta_1)h\big)V_1 \\ \frac{dV_2}{dt} = \alpha p_2 V_1 - \big(\mu + (1-\eta_2)h\big)V_2 \\ \frac{dE}{dt} = \big(S + (1-\eta_1)V_1 + (1-\eta_2)V_2\big)h - (\mu + e)E \\ \frac{dI_a}{dt} = \rho e E - (\mu + r_a)I_a \\ \frac{dI_s}{dt} = (1-\rho)eE - (r_s + \mu + d + \delta)I_s \\ \frac{dQ}{dt} = \delta I_s - (\mu + d + q_h + r_q)Q \\ \frac{dH}{dt} = q_h Q - (\mu + d + r_h)H \\ \frac{dR}{dt} = r_a I_a + r_s I_s + r_q Q + r_h H - \mu R, \end{cases} \tag{2}$$

with initial conditions

$S(0) \geq 0$, $V_1(0) \geq 0$, $V_2(0) \geq 0$, $E(0) \geq 0$, $I_a(0) \geq 0$, $I_s(0) \geq 0$, $Q(0) \geq 0$, $H(0) \geq 0$ and $R(0) \geq 0$.

3. Model analysis

In this section, positivity of solution, the invariant region, disease-free equilibrium, reproduction number, stability analysis , endemic equilibrium point, bifurcation and sensitivity analysis are discussed.

3.1 Positivity and boundedness of the solutions

Since each component of the given model system considers a human population, it is necessary to show that all variables $S(t), V_1(t), V_2(t), E(t), I_a(t), I_s(t), Q(t), H(t)$ and $R(t)$ are positive for all $t > 0$.

Theorem 3.1.1. *If* $S(0) \geq 0$, $V_1(0) \geq 0$, $V_2(0) \geq 0$, $E(0) \geq 0$, $I_a(0) \geq 0$, $I_s(0) \geq 0$, $Q(0) \geq 0$, $H(0) \geq 0$ *and* $R(0) \geq 0$, *then the solution set* $\{S(t), V_1(t), V_2(t), E(t), I_a(t), I_s(t), Q(t), H(t), R(t)\}$ *of the model* (2) *consists of positive members for all* $t > 0$.

Proof. From the first equation of system (2), we have

$$\frac{dS}{dt} = \pi - (p_1 + \mu + h)S.$$

This leads to,

$$\frac{dS}{dt} \geq -(p_1 + \mu + h)S.$$

And hence,

$$\frac{dS}{S} \geq -(p_1 + \mu + h)dt,$$

Upon integration, we obtain,

$$S(t) \geq S(0) \exp\left(-\int_0^t (p_1 + \mu + h)du\right) \geq 0,$$

Thus, $S(t) \geq 0$.

Similarly, it can be shown that the other equations of system (2) are positive for all $t > 0$. Hence, the state variables of the system are all positive for all $t > 0$. □

Theorem 3.1.2. *The feasible solution set* $\{S, V_1, V_2, E, I_a, I_s, Q, H, R\}$ *of the model* (2) *with the given initial condition remains bounded in the region* $\Omega = \{(S, V_1, V_2, E, I_a, I_s, Q, H, R) \in \mathbb{R}^9_+ : 0 \leq N \leq \frac{\pi}{\mu}\}$.

Proof. Differentiating N in equation (1) with respect to t we obtain;

$$\frac{dN}{dt} = \frac{dS}{dt} + \frac{dV_1}{dt} + \frac{dV_2}{dt} + \frac{dE}{dt} + \frac{dI_a}{dt} + \frac{dI_s}{dt} + \frac{dQ}{dt} + \frac{dH}{dt} + \frac{dR}{dt}. \tag{3}$$

Using system (2) and evaluating at (3) gives us;

$$\frac{dN}{dt} = \pi - \mu N - d(I_s + Q) - H(\mu + d).$$

Since the state variables of system I_s, Q and H are positive for all $t \geq 0$ we have

$$\frac{dN}{dt} \leq \pi - \mu N, \tag{4}$$

in which N is asymptotically bounded

$$i.e. \quad 0 \leq N \leq \frac{\pi}{\mu}.$$

This completes the proof. □

3.2 Reproduction number, existence and stability analysis of equilibria

3.2.1 Disease-free equilibrium point

In this subsection, we determine the equilibrium point at which there is no disease in the population (i.e. $I_a = I_s = Q = H = E = R = 0$) by letting the right hand side of system (2) to zero. We get:

$$\begin{aligned} E_{dfe} &= (S^*, V_1^*, V_2^*, E^*, I_a^*, I_s^*, Q^*, H^*, R^*)\,, \\ &= \left(\frac{\pi}{p_1+\mu}, \frac{p_1\pi}{(p_1+\mu)(\mu+\alpha p_2)}, \frac{\pi\alpha p_1 p_2}{\mu(p_1+\mu)(\mu+\alpha p_2)}, 0, 0, 0, 0, 0, 0\right). \end{aligned} \tag{5}$$

Remark 1. *In* (5)*, when there is no vaccination, i.e., $p_1 = 0$, the disease-free equilibrium will be reduced to a fully susceptible disease-free state given by*

$$\begin{aligned} E_0 &= (S^*, V_1^*, V_2^*, E^*, I_a^*, I_s^*, Q^*, H^*, R^*)\,, \\ &= \left(\frac{\pi}{\mu}, 0, 0, 0, 0, 0, 0, 0, 0\right). \end{aligned} \tag{6}$$

If $p_1 = 1$ we get a disease-free equilibrium in which every susceptible individual is vaccinated with the first dose, which can be expressed by

$$\begin{aligned} E_{01} &= (S^*, V_1^*, V_2^*, E^*, I_a^*, I_s^*, Q^*, H^*, R^*)\,, \\ &= \left(\frac{\pi}{1+\mu}, \frac{\pi}{(1+\mu)(\mu+\alpha)}, \frac{\pi\alpha}{\mu(1+\mu)(\mu+\alpha)}, 0, 0, 0, 0, 0, 0\right). \end{aligned} \tag{7}$$

3.2.2 Reproduction number

The basic reproduction number (R_0) is the average number of secondary cases produced by one primary infection during the infectious period in a fully susceptible population and the control reproduction number (in our case denoted by R_v) is used to represent the same quantity for a system incorporating control (or intervention) strategies [12]. We will use the next generation matrix method [11] to find the basic and control reproduction number.

Let the matrix for new infection appearance at the infected compartment be given by $\mathcal{F}$,

$$\mathcal{F} = \begin{bmatrix} E \\ I_a \\ I_s \\ Q \\ H \end{bmatrix} \begin{bmatrix} \big(S + (1-\eta_1)V_1 + (1-\eta_2)V_2\big)h \\ 0 \\ 0 \\ 0 \\ 0 \end{bmatrix}, \tag{8}$$

and the matrix of other transactions at each of the infected compartments can be represented by $\mathcal{V}$, and is given by

$$\mathcal{V} = \begin{bmatrix} E \\ I_a \\ I_s \\ Q \\ H \end{bmatrix} = \begin{bmatrix} (\mu+e)E \\ (\mu+r_a)I_a - \rho eE \\ (r_s+\mu+d+\delta)I_s - (1-\rho)eE \\ (\mu+d+r_h+r_a)Q - \delta I_s \\ (\mu+d+r_h)H - q_h Q \end{bmatrix}. \tag{9}$$

Now finding the Jacobian of $\mathcal{F}$ and $\mathcal{V}$, we get matrices F (only the first row, nonzero row) and V written as;

$$F = \begin{bmatrix} 0 & (S + (1-\eta_1)V_1 + (1-\eta_2)V_2)\frac{\partial h}{\partial I_a} & (S + (1-\eta_1)V_1 + (1-\eta_2)V_2)\frac{\partial h}{\partial I_s} & 0 & 0 \end{bmatrix}, \tag{10}$$

where,

$$\frac{\partial h}{\partial I_a} = \frac{\beta\tau(N-(Q+H)) - \beta(\tau I_a + I_s)}{(N-(Q+H))^2} \tag{11}$$

$$\frac{\partial h}{\partial I_s} = \frac{\beta(N-(Q+H)) - \beta(\tau I_a + I_s)}{(N-(Q+H))^2} \tag{12}$$

and

$$V = \begin{bmatrix} (\mu+e) & 0 & 0 & 0 & 0 \\ -\rho e & (\mu+r_a) & 0 & 0 & 0 \\ -(1-\rho)e & 0 & (r_s+\mu+d+\delta) & 0 & 0 \\ 0 & 0 & -\delta & (\mu+d+r_h+r_a) & 0 \\ 0 & 0 & 0 & -q_h & (\mu+d+r_h) \end{bmatrix}. \tag{13}$$

The control reproduction number is given by $R_v = \nu(F(E_v) \times V^{-1})$. Where ν is the spectral radius of the matrix $F(E_v) \times V^{-1}$. Thus R_v, can be written as:

$$R_v = \frac{(\mu(\mu+\alpha p_2) + (1-\eta_1)p_1\mu + (1-\eta_2)\alpha p_1 p_2)}{(\mu+e)(\mu+p_1)(\mu+\alpha p_2)} \left(\frac{\rho e \beta \tau}{\mu+r_a} + \frac{(1-\rho)e\beta}{r_s+\mu+d+\delta} \right). \tag{14}$$

The basic reproduction number, R_0 is obtained by setting $p_1 = p_2 = 0$ in (14) and is given by:

$$R_0 = \frac{\rho e \beta \tau}{(\mu+e)(\mu+r_a)} + \frac{(1-\rho)e\beta}{(\mu+e)(\mu+r_s+d+\delta)}. \tag{15}$$

We can rewrite equation (14) in terms of R_0 as;

$$R_v = \left(\frac{\mu(\mu+\alpha p_2) + (1-\eta_1)p_1\mu + (1-\eta_2)\alpha p_1 p_2}{(p_1+\mu)(\mu+\alpha p_2)} \right) R_0. \tag{16}$$

Remark 2. *If $\eta_1 = \eta_2 = 0$, then $R_v = R_0$. Otherwise ($0 < \eta_1, \eta_2 \leq 1$) $R_v < R_0$.*

In system (2), the solution for the state variables Q, H and R can easily be solved from other variables in the system and they does not affect them, therefore in the following subsections we restrict our mathematical analysis to the following system of equations.

$$\begin{cases} \frac{dS}{dt} = \pi - \big(p_1+\mu+h\big)S \\ \frac{dV_1}{dt} = p_1 S - \big(\alpha p_2 + \mu + (1-\eta_1)h\big)V_1 \\ \frac{dV_2}{dt} = \alpha p_2 V_1 - \big(\mu + (1-\eta_2)h\big)V_2 \\ \frac{dE}{dt} = \big(S + (1-\eta_1)V_1 + (1-\eta_2)V_2\big)h - (\mu+e)E \\ \frac{dI_a}{dt} = \rho e E - (\mu+r_a)I_a \\ \frac{dI_s}{dt} = (1-\rho)eE - (r_s+\mu+d+\delta)I_s \end{cases} \tag{17}$$

3.2.3 Local stability of disease-free equilibrium

Theorem 3.2.1. *The disease-free equilibrium, E_{dfe} is locally asymptotically stable if $R_v < 1$ and unstable if $R_v > 1$.*

Proof. The Jacobian matrix of the system (17) is given by:

$$J = \begin{bmatrix} -(p_1+\mu+h) & 0 & 0 & 0 & -\frac{\partial h}{\partial I_a}S & -\frac{\partial h}{\partial I_s}S \\ p_1 & -(\mu+\alpha p_2+(1-\eta_1)h) & 0 & 0 & -(1-\eta_1)V_1\frac{\partial h}{\partial I_a} & -(1-\eta_1)V_1\frac{\partial h}{\partial I_s} \\ 0 & \alpha p_2 & -(\mu+(1-\eta_2)h) & 0 & -(1-\eta_2)V_2\frac{\partial h}{\partial I_a} & -(1-\eta_2)V_2\frac{\partial h}{\partial I_s} \\ h & (1-\eta_1)h & (1-\eta_2)h & -(\mu+e) & H_1 & H_2 \\ 0 & 0 & 0 & \rho e & -(\mu+r_a) & 0 \\ 0 & 0 & 0 & (1-\rho)e & 0 & -(r_s+\mu+d+\delta) \end{bmatrix}, \tag{18}$$

where

$$\begin{aligned} H_1 &= \tfrac{\partial h}{\partial I_a} \times (S+(1-\eta_1)V_1+(1-\eta_2)V_2) \\ H_2 &= \tfrac{\partial h}{\partial I_s} \times (S+(1-\eta_1)V_1+(1-\eta_2)V_2), \end{aligned}$$

and $\frac{\partial h}{\partial I_a}$ and $\frac{\partial h}{\partial I_s}$ are as in equations (11) and (12).

The Jacobian matrix (18) evaluated at the disease-free equilibrium E_v is given by:

$$J(E_v) = \begin{bmatrix} -(\mu+p_1) & 0 & 0 & 0 & \frac{\partial h}{\partial I_a}(E_v)S^* & \frac{\partial h}{\partial I_s}(E_v)S^* \\ p_1 & -(\mu+\alpha p_2) & 0 & 0 & -(1-\eta_1)\frac{\partial h}{\partial I_a}(E_v)V_1^* & -(1-\eta_1)\frac{\partial h}{\partial I_s}(E_v)V_1^* \\ 0 & \alpha p_2 & -\mu & 0 & -(1-\eta_2)\frac{\partial h}{\partial I_a}(E_v)V_2^* & -(1-\eta_2)\frac{\partial h}{\partial I_s}(E_v)V_2^* \\ 0 & 0 & 0 & -(\mu+e) & H_1^* & H_2^* \\ 0 & 0 & 0 & \rho e & -(\mu+r_a) & 0 \\ 0 & 0 & 0 & (1-\rho)e & 0 & -(r_s+\mu+d+\delta) \end{bmatrix}, \tag{19}$$

where

$$\begin{aligned} \tfrac{\partial h}{\partial I_a}(E_v) &= \tfrac{\beta\tau\mu(p_1+\mu)(\mu+\alpha p_2)}{\mu\pi(\mu+\alpha p_2)+p_1\pi\mu+\pi\alpha p_1 p_2} \\ \tfrac{\partial h}{\partial I_s}(E_v) &= \tfrac{\beta\mu(p_1+\mu)(\mu+\alpha p_2)}{\mu\pi(\mu+\alpha p_2)+p_1\pi\mu+\pi\alpha p_1 p_2} \\ H_1^* &= \beta\tau\tfrac{\mu(\mu+\alpha p_2)+\mu(1-\eta_1)p_1+(1-\eta_2)p_1p_2\alpha}{(p_1+\mu)(\mu+\alpha p_2)} \\ H_2^* &= \beta\tfrac{\mu(\mu+\alpha p_2)+\mu(1-\eta_1)p_1+(1-\eta_2)p_1p_2\alpha}{(p_1+\mu)(\mu+\alpha p_2)}, \end{aligned}$$

and its characteristic equation is:

$$((\mu+\lambda)(\mu+p_1+\lambda)(\mu+\alpha p_2+\lambda))\left(-\lambda^3-B_1\lambda^2+B_2\lambda+B_3\right)=0, \tag{20}$$

where

$$\begin{aligned} B_1 =& r_s+3\mu+d+\delta+r_a+e, \\ B_2 =& (1-\rho)eH_2^*-(r_s+\mu+d+\delta)(2\mu+r_a+e)+\rho eH_1^*-(\mu+e)(\mu+r_a), \\ B_3 =& (1-\rho)e(\mu+r_a)H_2^*-(r_s+\mu+d+\delta)((\mu+e)(\mu+r_a)-\rho eH_1^*). \end{aligned}$$

From (20) we have the roots given by $\lambda_1 = -\mu$, $\lambda_2 = -(\mu+\alpha p_2)$, $\lambda_3 = -(\mu+p_1)$ and $-\lambda^3-B_1\lambda^2+B_2\lambda+B_3=0$. By Descartes' rule of sign, the roots of the later equation will be negative if $B_2<0$ and $B_3<0$.

Let write the equation for R_v in (14) in terms of H_1^* and H_2^* as:

$$R_v = \frac{\rho e}{(\mu+r_a)(\mu+e)}H_1^* + \frac{(1-\rho)e}{(\mu+r_s+d+\delta)(\mu+e)}H_2^*.$$

Suppose $R_v<1$, which implies

$$\rho e(\mu+r_s+d+\delta)H_1^*+(1-\rho)e(\mu+r_a)H_2^* < (\mu+e)(\mu+r_a)(\mu+r_s+d+\delta).$$

Therefore,

$$\rho e(\mu + r_s + d + \delta)H_1^* < (\mu + e)(\mu + r_a)(\mu + r_s + d + \delta),$$

and

$$(1-\rho)e(\mu + r_a)H_2^* < (\mu + e)(\mu + r_a)(\mu + r_s + d + \delta) < (\mu + r_s + d + \delta)(\mu + r_a)(2\mu + r_a + e),$$

which are equivalently written as

$$\begin{aligned} \rho e H_1^* - (\mu + e)(\mu + r_a) &< 0 \\ (1-\rho)e H_2^* - (\mu + e)(2\mu + r_a + e) &< 0. \end{aligned} \tag{21}$$

From the inequalities in (21), we summarize that: $B_2 < 0$ if $R_v < 1$. And it can also be shown that $B_3 < 0$ whenever $R_v < 1$. Therefore, the disease-free equilibrium E_{dfe} is locally asymptotically stable if $R_v < 1$. For $R_v > 1$, B_2 will be greater than zero, therefore we will have at least one positive eigenvalue, therefore E_{dfe} will be unstable. □

3.2.4 Global stability of disease-free equilibrium point when $R_v < 1$

To investigate the global stability of disease-free equilibrium, we use the technique implemented by Castillo-Chavez et al. [7]. We write the model system (17) as

$$\begin{aligned} \frac{dU}{dt} &= F(U, Z) \\ \frac{dZ}{dt} &= G(U, Z) \\ G(U, 0) &= 0 \end{aligned}$$

where U stands for the uninfected individual, that is, $U = (S, V_1, V_2)^T \in \mathbb{R}^3_+$ and Z for the infected individuals ,that is, $Z = (E, I_a, I_s)^T \in \mathbb{R}^3_+$. The disease free equilibrium point of the model is denoted by $E_v = (U_0, 0)$. For $R_v < 1$, for which the disease free equilibrium point is locally asymptotically stable the following two conditions are sufficient to guarantee the global stability of disease free equilibrium point $(U_0, 0)$.

(H1) For $\dfrac{du}{dt} = F(U, 0)$, U_0 is globally asymptotically stable.

(H2) $G(U, Z) = AZ - \tilde{G}(U, Z)$, where $\tilde{G}(U, Z) \geq 0$ for all $(U, Z) \in \Omega$

where $A = D_I G(U_0, 0)$ is a M-matrix (the off diagonal elements of A are nonnegative) and Ω is the region where the model makes biological sense.

Theorem 3.2.2. *The point $E_v = (U_0, 0)$ is globally asymptotically stable provided that $R_v < 1$ and the conditions expressed in (H1) and (H2) are satisfied.*

Proof. For condition (H1) from the system (17) we can get $F(U, Z)$

$$F(U, Z) = \begin{bmatrix} \pi - \big(p_1 + \mu + h\big)S \\ p_1 S - \big(\alpha p_2 + \mu + (1-\eta_1)h\big)V_1 \\ \alpha p_2 V_1 - \big(\mu + (1-\eta_2)h\big)V_2 \end{bmatrix}$$

Hence,

$$F(U, 0) = \begin{bmatrix} \pi - (p_1 + \mu)S \\ p_1 S - (\alpha p_2 + \mu)V_1 \\ \alpha p_2 V_1 - \mu V_2 \end{bmatrix}$$

It is obvious that $U_0 = (\frac{\pi}{p_1+\mu}, \frac{p_1\pi}{(p_1+\mu)(\mu+\alpha p_2)}, \frac{\pi\alpha p_1 p_2}{\mu(p_1+\mu)(\mu+\alpha p_2)}, 0)$ is globally asymptotically stable for $F(U,0)$ as $U \to U_0$ when $t \to \infty$.

For condition (H2) from the system (17) we can get $G(U,Z)$

$$G(U,Z) = \begin{bmatrix} \big(S + (1-\eta_1)V_1 + (1-\eta_2)V_2\big)h - (\mu+e)E \\ \rho eE - (\mu + r_a)I_a \\ (1-\rho)eE - (r_s + \mu + d + \delta)I_s \end{bmatrix}$$

and

$$A = \begin{bmatrix} -(\mu+e) & \big(S^* + (1-\eta_1)V_1^* + (1-\eta_2)V_2^*\big)\frac{\beta\tau}{N^*} & \big(S^* + (1-\eta_1)V_1^* + (1-\eta_2)V_2^*\big)\frac{\beta}{N^*} \\ e\rho & -(\mu + r_a) & 0 \\ (1-\rho)e & 0 & -(r_s + \mu + d + \delta) \end{bmatrix}$$

where,

$$N^* = S^* + V_1^* + V_2^*$$

We have

$$\begin{aligned} \tilde{G}(U,Z) &= AZ - G(U,Z) \\ &= \begin{bmatrix} \tilde{G}_1(U,Z) \\ \tilde{G}_2(U,Z) \\ \tilde{G}_3(U,Z) \end{bmatrix} = \begin{bmatrix} \beta(\tau I_a + I_s)\left[\frac{S^*+(1-\eta_1)V_1^*+(1-\eta_2)V_2^*}{N*} - \left(\frac{S+(1-\eta_1)V_1+(1-\eta_2)V_2}{N-(Q+H)}\right)\right] \\ 0 \\ 0 \end{bmatrix} \end{aligned}$$

which leads to $\tilde{G}(U,Z) \geq 0$ for all $(U,Z) \in \Omega$. Hence both the conditions (H1) and (H2) are satisfied. Therefore, the disease-free equilibrium point is globally asymptotically stable for $R_v < 1$. □

3.2.5 Existence of endemic equilibrium

By equating the system (2) to zero, we get the endemic equilibrium in terms of the force of infection h and we denote it by

$$E_{end} = \Big(S^e, V_1^e, V_2^e, E^e, I_a^e, I_s^e, Q^e, H^e, R^e\Big),$$

the components of E_{end} are given as follows:

$$\begin{aligned}
S^e &= \frac{\pi}{p_1 + \mu + h^e}, \\
V_1^e &= \frac{p_1\pi}{(p_1+\mu+h^e)(\alpha p_2 + \mu + (1-\eta_1)h^e)}, \\
V_2^e &= \frac{p_1 p_2 \alpha\pi}{(p_1+\mu+h^e)(\alpha p_2 + \mu + (1-\eta_1)h^e)(\mu + (1-\eta_2)h^e)}, \\
E^e &= \frac{h^e\pi\big[(\mu+(1-\eta_2)h^e)(\alpha p_2 + \mu + (1-\eta_1)h^e) + p_1(1-\eta_1)(\mu+(1-\eta_2)h^e) + \alpha p_1 p_2(1-\eta_2)\big]}{(\mu+e)(p_1+\mu+h^e)(\alpha p_2 + \mu + (1-\eta_1)h^e)(\mu+(1-\eta_2)h^e)}, \\
I_a^e &= \frac{\rho e h^e\pi\big[(\mu+(1-\eta_2)h^e)(\alpha p_2 + \mu + (1-\eta_1)h^e) + p_1(1-\eta_1)(\mu+(1-\eta_2)h^e) + \alpha p_1 p_2(1-\eta_2)\big]}{(\mu+r_a)(\mu+e)(p_1+\mu+h^e)(\alpha p_2 + \mu + (1-\eta_1)h^e)(\mu+(1-\eta_2)h^e)}, \\
I_s^e &= \frac{(1-\rho)e h^e\pi\big[(\mu+(1-\eta_2)h^e)(\alpha p_2 + \mu + (1-\eta_1)h^e) + p_1(1-\eta_1)(\mu+(1-\eta_2)h^e) + \alpha p_1 p_2(1-\eta_2)\big]}{(r_s+\mu+d+\delta)(\mu+e)(p_1+\mu+h^e)(\alpha p_2 + \mu + (1-\eta_1)h^e)(\mu+(1-\eta_2)h^e)}, \\
Q^e &= \frac{\delta}{\mu + d + q_h + r_q} \times I_s^e, \\
H^e &= \frac{q_h}{\mu + d + r_h} \times Q^e, \\
R^e &= \frac{r_a I_a^e + r_s I_s^e + r_q Q^e + r_h H^e}{\mu},
\end{aligned}$$

where h^e is the positive root of the equation

$$g(h^e) = A(h^e)^3 + B(h^e)^2 + Ch^e + D = 0, \tag{22}$$

obtained from

$$h^e = \frac{\beta(\tau I_a^e + I_s^e)}{(S^e + V_1^e + V_2^e + E^e + I_a^e + I_s^e + R^e)},$$

and the coefficients in equation (22) are given by

$$A = (1-\eta_1)(1-\eta_2)$$

$$B = \frac{J_1 + \Big(\mu(\mu+\alpha p_2)(p_1+\mu)(1-\eta_1)(1-\eta_2)\Big)(1-R_v)}{\mu(\mu+\alpha p_2) + (1-\eta_1)p_1\mu + (1-\eta_2)\alpha p_1 p_2}$$

$$C = \frac{J_2 + \Big((p_1+\mu)\big(\mu^2(1-\eta_1)(\mu+\alpha p_2) + \mu(1-\eta_2)(\mu+\alpha p_2)^2\big) + p_1\mu(1-\eta_1)(\alpha p_2+\mu)(p_1+\mu)(1-\eta_2)\Big)(1-R_v)}{\mu(\mu+\alpha p_2) + (1-\eta_1)p_1\mu + (1-\eta_2)\alpha p_1 p_2}$$

$$D = \mu(p_1+\mu)(\alpha p_2+\mu)(1-R_v),$$

where,

$$\begin{aligned} J_1 &= \mu(\mu+\alpha p_2)(\mu(1-\eta_1) + (\mu+\alpha p_2)(1-\eta_2)) + p_1\mu(1-\eta_1)^2(\mu + (p_1+\mu)(1-\eta_2) + (\alpha p_2+\mu)) \\ &\quad + \alpha p_1 p_2(1-\eta_2)(\mu(1-\eta_1) + (p_1+\mu)(1-\eta_1)(1-\eta_2) + (\alpha p_2+\mu)(1-\eta_2)) \\ J_2 &= \mu^2(\alpha p_2+\mu)^2 + p_1\mu^2(1-\eta_1)((p_1+\mu)(1-\eta_1) + (\alpha p_2+\mu)) \\ &\quad + \mu\alpha p_1 p_2(1-\eta_2)((1-\eta_1)(p_1+\mu) + (\alpha p_2+\mu) + (\alpha p_2+\mu)(p_1+\mu)(1-\eta_1)). \end{aligned}$$

It can easily be seen that $A > 0$. If $R_v > 1$ then $D < 0$, therefore $h(0) < 0$. Additionally $\lim_{h^e \to \infty} g(h^e) > 0$. Therefore, from the continuity of g, there exists at least one positive h_*^e such that $g(h_*^e) = 0$ and hence there will be at least one endemic equilibrium of the model system (2). On the other hand, if $R_v < 1$, then $B > 0, C > 0$ and $D > 0$ then by Descartes' rule of sign, (22) has no positive real root, which proves that there is no endemic equilibrium point when $R_v < 1$. From the above discussion, we can state the following theorem.

Theorem 3.2.3. *If $R_v > 1$, there exists at least one endemic equilibrium point for the model system* (2) *and there is no endemic equilibrium point for the model system* (2) *when $R_v < 1$.*

3.3 Bifurcation analysis

We determine the occurrence of a transcritical bifurcation at $R_v = 1$ by adopting the well–known approach based on the general center manifold theory [6]. In short, it establishes that the normal form representing the dynamics of the system on the central manifold is given by:

$$\dot{u} = au^2 + b\beta u,$$

where

$$a = \sum_{k,i,j=1}^{n} \nu_k \omega_i \omega_j \frac{\partial^2 f_k}{\partial x_i \partial x_j}(E_v, \beta^*), \tag{23}$$

and

$$b = \sum_{k,i=1}^{n} \nu_k \omega_i \frac{\partial^2 f_k}{\partial x_i \partial \beta}(E_v, \beta^*). \tag{24}$$

Note that β has been chosen as a bifurcation parameter and β^* is its critical value, f represents the right–hand side of the system (17), x represents the state variable vector, $x = (x_1, x_2, x_3, x_4, x_5, x_6) = (S, V_1, V_2, E, I_a, I_s)$,

ν and ω are the left and right eigenvectors corresponding to the zero eigenvalue of the Jacobian matrix at the disease-free equilibrium and the critical value, i.e., at E_v and $\beta = \beta^*$.

Observe that $R_v = 1$ is equivalent to $\beta = \beta^*$, with

$$\beta^* = \frac{(\mu+e)(\mu+p_1)(\mu+\alpha p_2)}{\mu(\mu+\alpha p_2)+(1-\eta_1)p_1\mu+(1-\eta_2)\alpha p_1 p_2} \times C,$$

where,

$$C = \frac{(\mu+r_a)(r_s+\mu+d+\delta)}{\rho e\tau(r_s+\mu+d+\delta)+(1-\rho)e(\mu+r_a)}$$

Thus, according to Theorem 4.1[6], the disease-free equilibrium is locally asymptotically stable if $\beta < \beta^*$, and it is unstable when $\beta > \beta^*$. The direction of the bifurcation occurring at $\beta = \beta^*$ can be derived from the sign of the coefficients (23) and (24). More precisely, if $a > 0$ (resp. $a < 0$) and $b > 0$, then at $\beta = \beta^*$ there is a backward (resp. forward) bifurcation.

By evaluating the Jacobian matrix of system (17) at E_v and $\beta = \beta^*$, we get

$$J(E_v,\beta^*) = \begin{bmatrix} -(\mu+p_1) & 0 & 0 & 0 & K_1 & K_4 \\ p_1 & -(\mu+\alpha p_2) & 0 & 0 & K_2 & K_5 \\ 0 & \alpha p_2 & -\mu & 0 & K_3 & K_6 \\ 0 & 0 & 0 & -(\mu+e) & H_1^* & H_2^* \\ 0 & 0 & 0 & \rho e & -(\mu+r_a) & 0 \\ 0 & 0 & 0 & (1-\rho)e & 0 & -(r_s+\mu+d+\delta) \end{bmatrix},$$

where

$$\begin{aligned} K_1 &= S^* \tfrac{\partial h}{\partial I_a}(E_v,\beta*) \\ K_2 &= -(1-\eta_1)V_1^* \tfrac{\partial h}{\partial I_a}(E_v,\beta*) \\ K_3 &= -(1-\eta_2)V_2^* \tfrac{\partial h}{\partial I_a}(E_v,\beta*) \\ K_4 &= S^* \tfrac{\partial h}{\partial I_s}(E_v,\beta*) \\ K_5 &= -(1-\eta_1)V_1^* \tfrac{\partial h}{\partial I_s}(E_v,\beta*) \\ K_6 &= -(1-\eta_2)V_2^* \tfrac{\partial h}{\partial I_s}(E_v,\beta*) \\ H_1^* &= \beta^*\tau \tfrac{\mu(\mu+\alpha p_2)+\mu(1-\eta_1)p_1+(1-\eta_2)p_1p_2\alpha}{(p_1+\mu)(\mu+\alpha p_2)} \\ H_2^* &= \beta^* \tfrac{\mu(\mu+\alpha p_2)+\mu(1-\eta_1)p_1+(1-\eta_2)p_1p_2\alpha}{(p_1+\mu)(\mu+\alpha p_2)} \end{aligned}$$

We observed that one of the eigenvalues of $J(E_v,\beta^*)$ is 0 and the remaining are negative. Hence, when $\beta = \beta^*$ (equivalently, when $R_v = 1$), the disease-free equilibrium is nonhyperbolic.

After some calculations we get:

$$\nu = (0,0,0,\nu_4,\frac{\nu_4 H_1^*}{\mu+r_a},\frac{\nu_4 H_2^*}{r_s+\mu+d+\delta}) \quad \text{and} \quad \omega = (\omega_1,\omega_2,\omega_3,1,\frac{e\rho}{\mu+r_a},\frac{e(1-\rho)}{r_s+\mu+d+\delta})^T,$$

where

$$\nu_4 = \frac{(\mu+r_a)^2(r_s+\mu+d+\delta)^2}{(\mu+r_a)^2(r_s+\mu+d+\delta)^2+H_1^* e\rho(r_s+\mu+d+\delta)^2+H_2^* e(1-\rho)(\mu+r_a)^2}$$

$$\omega_1 = \frac{K_1 e\rho(r_s+\mu+d+\delta)+K_4 e(1-\rho)(\mu+r_a)}{(\mu+p_1)(\mu+r_a)(r_s+\mu+d+\delta)} < 0$$

$$\omega_2 = \frac{p_1\omega_1(\mu+r_a)(r_s+\mu+d+\delta)+K_2 e\rho(r_s+\mu+d+\delta)+K_5 e(1-\rho)(\mu+r_a)}{(\mu+\alpha p_2)(\mu+r_a)(r_s+\mu+d+\delta)} < 0$$

$$\omega_3 = \frac{p_2\alpha\omega_2\mu(\mu+r_a)(r_s+\mu+d+\delta)+K_3 e\rho(r_s+\mu+d+\delta)+K_6 e(1-\rho)(\mu+r_a)}{\mu(\mu+r_a)(r_s+\mu+d+\delta)} < 0.$$

are a left and right eigenvector associated with the zero eigenvalue, respectively, such that $\nu \cdot \omega = 1$. Now we can explicitly compute the coefficients a and b. Considering only the nonzero components of the eigenvectors and computing the corresponding second derivative of f, it follows that:

$$\begin{aligned}
a &= \sum_{k,i,j=1}^{6} \nu_k \omega_i \omega_j \frac{\partial^2 f_k}{\partial x_i \partial x_j}(E_v, \beta^*) \\
&= 2[\nu_4\omega_1(\omega_5 \frac{\partial^2 f_4}{\partial S \partial I_a}(E_v, \beta^*) + \omega_6 \frac{\partial^2 f_4}{\partial S \partial I_s}(E_v, \beta^*)) + \nu_4\omega_2(\omega_5 \frac{\partial^2 f_4}{\partial V_1 \partial I_a}(E_v, \beta^*) + \omega_6 \frac{\partial^2 f_4}{\partial V_1 \partial I_s}(E_v, \beta^*)) \\
&\quad + \nu_4\omega_3(\omega_5 \frac{\partial^2 f_4}{\partial V_2 \partial I_a}(E_v, \beta^*) + \omega_6 \frac{\partial^2 f_4}{\partial V_2 \partial I_a}(E_v, \beta^*))] \\
&= \frac{2\beta^*}{(\mu + r_a)(r_s + \mu + d + \delta)} \Big[e\omega_1(\tau\rho(r_s + \mu + d + \delta) + (1-\rho)(\mu + ra)) \\
&\quad + e\omega_2(\rho\tau(1-\eta_1)(r_s + \mu + d + \delta) + (1-\rho)(1-\eta_1)(\mu + r_a)) \\
&\quad + e\omega_3(\rho\tau(1-\eta_2)(r_s + \mu + d + \delta) + (1-\rho)(1-\eta_2)(\mu + r_a)) \Big]
\end{aligned}$$

Since ω_1, ω_2 and ω_3 are negative, $a < 0$.
And

$$\begin{aligned}
b &= \sum_{k,i=1}^{6} \nu_k \omega_i \frac{\partial^2 f_k}{\partial x_i \partial \beta}(E_v, \beta^*) \\
&= \nu_4 \Big[\omega_2 \frac{\partial^2 f_4}{\partial V_1 \partial \beta}(E_v, \beta^*) + \omega_2 \frac{\partial^2 f_4}{\partial V_2 \partial \beta}(E_v, \beta^*) + \omega_2 \frac{\partial^2 f_4}{\partial I_a \partial \beta}(E_v, \beta^*) + \omega_2 \frac{\partial^2 f_4}{\partial I_s \partial \beta}(E_v, \beta^*) \Big] \\
&= \nu_4 \Big[\frac{e\rho\tau}{\mu + r_a}(S^* + (1-\eta_1)V_1^* + (1-\eta_2)V_2^*) + \frac{e(1-\rho)}{r_s + \mu + d + \delta}(S^* + (1-\eta_2)V_1^* + (1-\eta_2)V_2^*) \Big] \\
&= \nu_4 (S^* + (1-\eta_1)V_1^* + (1-\eta_2)V_2^*) \Big[\frac{e\rho\tau}{\mu + r_a} + \frac{e(1-\rho)}{r_s + \mu + d + \delta} \Big] > 0
\end{aligned}$$

Since $a < 0$ and $b > 0$, by the result of Castillo-Chavez and Song [6], model (17) exhibits a forward bifurcation at $R_v = 1$(see Figure 5). We summarize the above discussion with the following theorem.

Theorem 3.3.1. *The endemic equilibrium point, E_{dfe} of the model system* (17)*, is locally asymptotically stable for $R_v > 1$ and the system exhibits forward(or transcritical) bifurcation at $R_v = 1$.*

3.4 Sensitivity analysis

In what follows, we investigate the sensitivity analysis for the control reproduction number R_v to identify the parameters that has high impact on disease expansion in the community. The sensitivity index with respect to a parameter X_i is given by a normalized forward sensitivity index [8],

$$\Gamma_{X_i}^{R_v} = \frac{\partial R_v}{\partial X_i} \times \frac{X_i}{R_v},$$

where, X_i represent the basic parameters.
Hence,

$$\Gamma_{e}^{R_v} = \frac{\partial R_v}{\partial e} \times \frac{e}{R_v} = \frac{\mu}{\mu + e} > 0,$$

$$\Gamma_{\eta_1}^{R_v} = \frac{\partial R_v}{\partial \eta_1} \times \frac{\eta}{R_v} = -\frac{p_1\mu}{(\mu+e)(\mu+p_1)(\mu+\alpha p_2)}\left(\frac{\rho e\beta\tau}{\mu+r_a} + \frac{(1-\rho)e\beta}{r_s+\mu+d+\delta}\right) \times \frac{\eta}{R_v} < 0,$$

$$\Gamma_{\eta_2}^{R_v} = \frac{\partial R_v}{\partial \eta_2} \times \frac{\eta_2}{R_v} = -\frac{\alpha p_1 p_2}{(\mu+e)(\mu+p_1)(\mu+\alpha p_2)}\left(\frac{\rho e\beta\tau}{\mu+r_a} + \frac{(1-\rho)e\beta}{r_s+\mu+d+\delta}\right) \times \frac{\eta_2}{R_v} < 0,$$

$$\Gamma_{p_1}^{R_v} = \frac{\partial R_v}{\partial p_1} \times \frac{p_1}{R_v} = -\frac{(\mu^2\eta_1 + \alpha\eta p_2\eta_2)}{(\mu+e)(\mu+p_1)^2(\mu+\alpha p_2)}\left(\frac{\rho e\beta\tau}{\mu+r_a} + \frac{(1-\rho)e\beta}{r_s+\mu+d+\delta}\right) \times \frac{p_1}{R_v} < 0,$$

$$\Gamma_{p_2}^{R_v} = \frac{\partial R_v}{\partial p_2} \times \frac{p_2}{R_v} = -\frac{\alpha^2 p_2(1-\mu)}{(\mu+e)(\mu+p_1)(\mu+\alpha p_2)^2}\left(\frac{\rho e\beta\tau}{\mu+r_a} + \frac{(1-\rho)e\beta}{r_s+\mu+d+\delta}\right) \times \frac{p_2}{R_v} < 0,$$

$$\Gamma_{\alpha}^{R_v} = \frac{\partial R_v}{\partial \alpha} \times \frac{\alpha}{R_v} = \frac{\mu p_1 p_2(\eta_1-\eta_2)}{(\mu+e)(\mu+p_1)(\mu+\alpha p_2)^2}\left(\frac{\rho e\beta\tau}{\mu+r_a} + \frac{(1-\rho)e\beta}{r_s+\mu+d+\delta}\right) \times \frac{\alpha}{R_v} < 0,$$

$$\Gamma_{\beta}^{R_v} = \frac{\partial R_v}{\partial \beta} \times \frac{\beta}{R_v} = 1 > 0,$$

$$\Gamma_{\tau}^{R_v} = \frac{\partial R_v}{\partial \tau} \times \frac{\alpha}{R_v} = \frac{(\mu(\mu+\alpha p_2) + \mu p_1(1-\eta_1) + \alpha p_1 p_2)\,(\rho e\beta)}{(\mu+e)(\mu+p_1)(\mu+\alpha p_2)(\mu+r_a)} \times \frac{\tau}{R_v} > 0,$$

$$\Gamma_{r_a}^{R_v} = \frac{\partial R_v}{\partial r_a} \times \frac{r_a}{R_v} = -\frac{(\mu(\mu+\alpha p_2) + \mu p_1(1-\eta_1) + \alpha p_1 p_2)\,(\rho e\beta\tau)}{(\mu+e)(\mu+p_1)(\mu+\alpha p_2)(\mu+r_a)^2} \times \frac{r_a}{R_v} < 0,$$

$$\Gamma_{r_s}^{R_v} = \frac{\partial R_v}{\partial r_s} \times \frac{r_s}{R_v} = -\frac{(\mu(\mu+\alpha p_2) + \mu p_1(1-\eta_1) + \alpha p_1 p_2)\,((1-\rho)e\beta)}{(\mu+e)(\mu+p_1)(\mu+\alpha p_2)(r_s+\mu+d+\delta)^2} \times \frac{r_s}{R_v} < 0,$$

$$\Gamma_{\delta}^{R_v} = \frac{\partial R_v}{\partial \delta} \times \frac{\delta}{R_v} = -\frac{(\mu(\mu+\alpha p_2) + \mu p_1(1-\eta_1) + \alpha p_1 p_2)\,((1-\rho)e\beta)}{(\mu+e)(\mu+p_1)(\mu+\alpha p_2)(r_s+\mu+d+\delta)^2} \times \frac{\delta}{R_v} < 0,$$

$$\Gamma_{d}^{R_v} = \frac{\partial R_v}{\partial d} \times \frac{d}{R_v} = -\frac{(\mu(\mu+\alpha p_2) + \mu p_1(1-\eta_1) + \alpha p_1 p_2)\,((1-\rho)e\beta)}{(\mu+e)(\mu+p_1)(\mu+\alpha p_2)(r_s+\mu+d+\delta)^2} \times \frac{d}{R_v} < 0.$$

We summarize the sensitivity analysis indices of the reproduction number with respect to some parameters in Table 1.

parameter	index
e	+ve
β	+ve
τ	+ve
η_1	-ve
η_2	-ve
p_1	-ve
p_2	-ve
α	-ve
r_a	-ve
r_s	-ve
δ	-ve
d	-ve

Table 1: Sensitivity index table

From Table1 the sensitivity indices with negative signs indicate that the value of R_v decreases when the parameter values are increased and the value of R_v increases when the parameter values are decreased, while sensitivity indices with positive signs indicate that the value of R_v increases when the parameter values are increased and the value of R_v decreases when the parameter values are decreased.

4. Numerical simulation and discussion

To justify the analytical results and explore additional important properties of the model, we fitted the model to real COVID-19 data of Ethiopia to fix the unknown parameters of the model and carried out a numerical simulation. In this section, we used the full model (2).

4.1 Parameter estimation

In this subsection, we will find the best values of unknown parameters in our model, with the so-called model fitting process. We used the real data of COVID-19 daily new cases and vaccinated population of Ethiopia from May 01, 2021 to January 31, 2022. We took the data which is available online by Our World in Data [19]. To fit the model to this data, we used the nonlinear curve fitting method with the help of 'lsqcurvefit', builtin MATLAB function. Some of the parameter values are estimated from literature: according to the data by Worldometer, the Ethiopian average life expectancy at birth for the year 2021 and the approximate total population is 67.8 and 114963588 respectively [27]. Therefore, the natural death rate of individuals per day is calculated as the reciprocal of the life expectancy at birth time days in a year, given by $\mu = \frac{1}{67.8\times 365}$. We approximated the recruitment rate from $\frac{\pi}{\mu} = N(0)$ (Initial population). Hence we found $\pi = \mu \times N(0) = 4646$ individuals per day. In the estimation process of the rest parameters the following initial conditions are used: from the data in Our World in Data we have $I_s(0) = 620, V_1(0) = 20385, R(0) = 946$ and $D(0) = 21$. Where $t = 0$ corresponds to May 01, 2021. According to WHO report 80% of COVID-19 infected individuals become asymptomatic. Therefore we estimated $I_a(0) = 620/0.8 = 775$. We assumed $E(0) = 1400$, which is approximately equal to the sum of the symptomatic and asymptomatic cases, and $V_1(0) = Q(0) = H(0) = 0$. Hence, the initial susceptible population is taken as $S(0) = N(0) - (V_1(0) + V_2(0) + E(0) + I_a(0) + I_s(0) + Q(0) + H(0) + R(0))$.

The best fit to the daily cumulative COVID-19 confirmed cases and vaccination through our model is shown in Figure 2. The estimated and calculated parameter values are given in Table 2. Using these parameters, we found $R_0 = 1.17$ and $R_v = 1.15$.

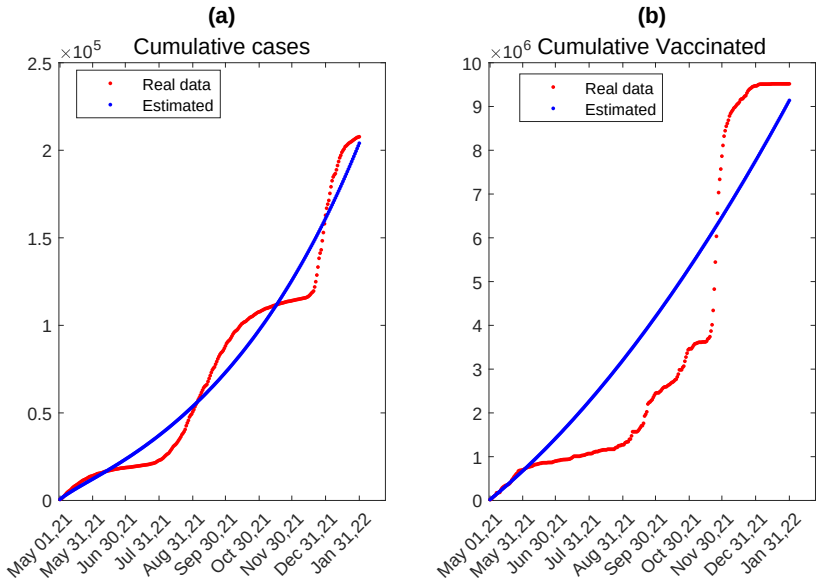

Figure 2: The fitted data to the reported cumulative cases (panel (a)) and cumulative vaccinated(panel (b)) using the model (2) for Ethiopia from May 01, 2021 to January 31, 2022.

Parameter	Description	Value	Sources
π	Recruitment rate	4646 $days^{-1}$	Calculated Sec.4.1
μ	Natural death rate	$\frac{1}{67.8\times365}$	Calculated Sec.4.1
p_1	First dose Vaccination rate	8.157×10^{-7} $days^{-1}$	Fitted
p_2	Second dose Vaccination rate	0.974 $days^{-1}$	Fitted
β	Transmission rate	0.513 $days^{-1}$	Fitted
τ	Infectivity factor for asymptomatic individuals	0.116	Fitted
η_1	Efficacy of first dose vaccine	0.8	Fitted
η_2	Efficacy of second dose vaccine	0.95	Fitted
α	Inverse of average time needed to take the second dose	0.14 $days^{-1}$	Fitted
ρ	fraction of infections that become asymptomatic	0.112	Fitted
e	Infection rate after incubation period	0.2071	Fitted
r_s	Recovery rate for individuals with symptom	1.89×10^{-7} $days^{-1}$	Fitted
r_a	Recovery rate for asymptomatic individuals	0.0148 $days^{-1}$	Fitted
r_q	Recovery rate for quarantined individuals	0.0356 $days^{-1}$	Fitted
r_h	Recovery rate for individuals in hospital	0.213 $days^{-1}$	Fitted
δ	Quarantine rate	0.453 $days^{-1}$	Fitted
d	Disease induced death rate	0.177 $days^{-1}$	Fitted
q_h	Hospitalization rate from quarantine	0.999 $days^{-1}$	Fitted

Table 2: Parameter description and their baseline values used in the model (2).

4.2 Local stability of disease-free and endemic equilibrium

Figure 3, panels (a) and (b) (for time interval $[9000, 30000]$) shows the local stability of the endemic equilibrium $E_{end} = [3.77 \times 10^{-7}, 225, 6.91 \times 10^5, 1.49 \times 10^4, 2.334 \times 10^4, 4.36 \times 10^3, 1.632 \times 10^3, 4.181 \times 10^3, 3.201 \times 10^7]$ for $R_v = 2.98 > 1$. Panels (c) and (d) portrays the stability of the disease free equilibrium,$E_{dfe} = [1.127 \times 10^8, 673.9, 2.2741 \times 10^6, 0, 0, 0, 0, 0, 0]$, for $R_v = 0.556 < 1$. These results support our analytical results in section 3 of Theorem 3.2.2 and 3.3.1. For better use of spacing and view we didn't include the plot for E compartment, but the dynamics of this state variable converges to its equilibrium point. The convergence to the endemic equilibrium is through damped oscillation, which may show the disease will be endemic in different times in the future. When $R_v = 1$ an exchange of stability (transcritical bifurcation) arises, *i.e.* for $R_v < 1$ there is no endemic equilibrium and the disease-free equilibrium is globally asymptotically stable and for $R_v > 1$ a stable endemic equilibrium appears whereas the disease-free equilibrium is unstable. This property is shown in Figure 5. From an epidemiological point of view, this means the disease may persist in the population for $R_v > 1$ and dies out for $R_v < 1$.

Remark 3. *In Figure 3, panels* (a) *and* (b) *at the beginning of the interval (i.e.,* $[0, 9000]$*) there is a relatively high peak, therefore in the plot with full interval the MATLAB suppresses the other peaks. Therefore, for better visualization of the long time interval behaviour of the model, we put the plot only for the interval* $[9000, 300000]$.

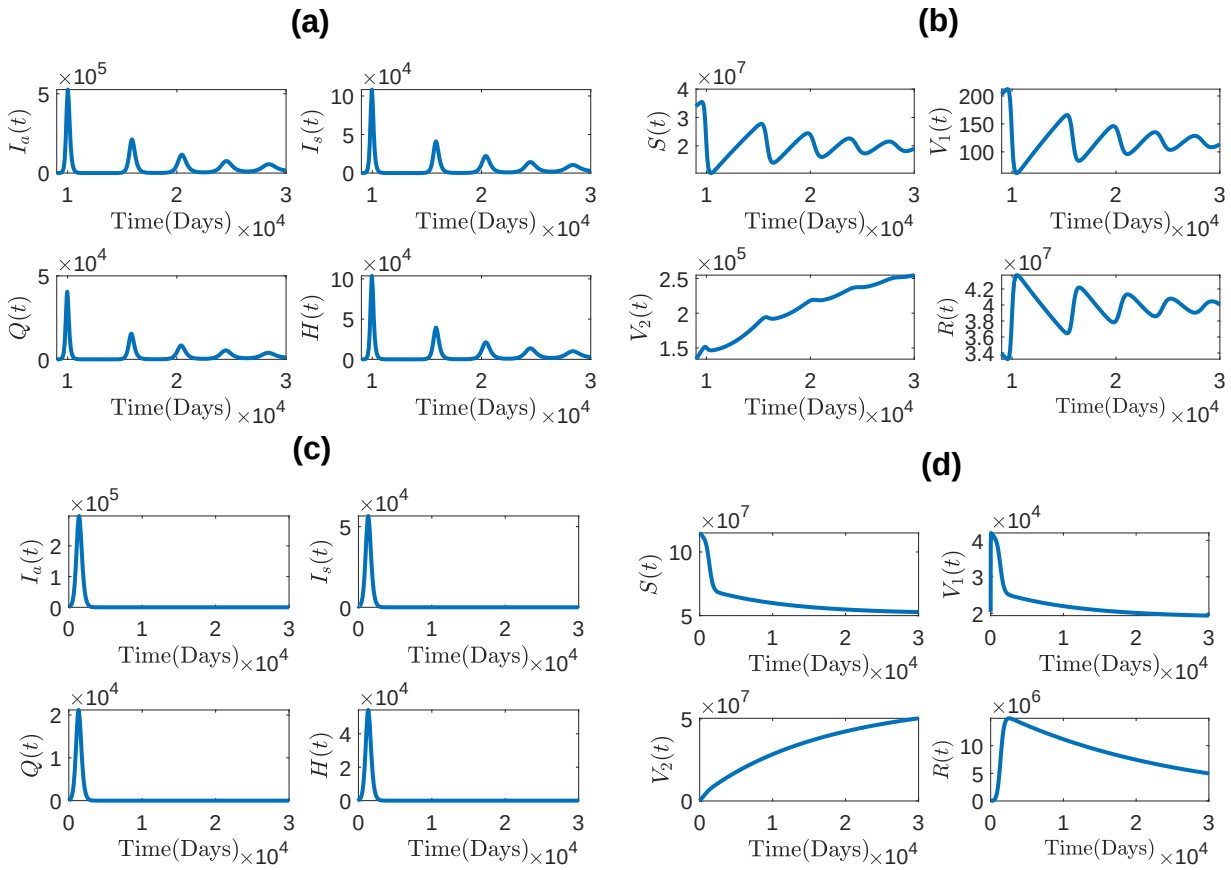

Figure 3: Local stability of the endemic equilibrium for $R_v = 2.98 > 1$(infected compartments, panels (a), and non infected compartments, panel (b)) and local stability of the disease free equilibrium for $R_v = 0.556 < 1$ (infected compartments, panel (c), and non infected compartments, panel (d).) $\tau_1 = 0.6$ and $p_1 = 5 \times 10^{-5}$ is used for panels $(a)\&(b)$ and $(c)\&(d)$ respectively and other parameter values are given in Table 2.

4.3 Variation of R_v with respect to some important parameters

An important parameter in modeling infectious disease transmission is the reproduction parameter which measures the potential spread of an infectious disease in a community, in our case we have a control reproduction parameter, R_v. In particular, if $R_v < 1$ the disease dies out and if $R_v > 1$ the disease persists in the population. Therefore reducing such parameter below the critical value $R_v = 1$ is important. In our model, reducing the transmission rate β and infectivity factor of asymptomatic individuals, τ will help reduce R_v from unity, Figure 4 panels (a) and (b). On the contrary increasing the first dose vaccination rate, p_1 will make R_v less than one, Figure 4 panel (c). Here it is worth to mention the influence of the second dose vaccination rate is low in varying the control reproduction number.

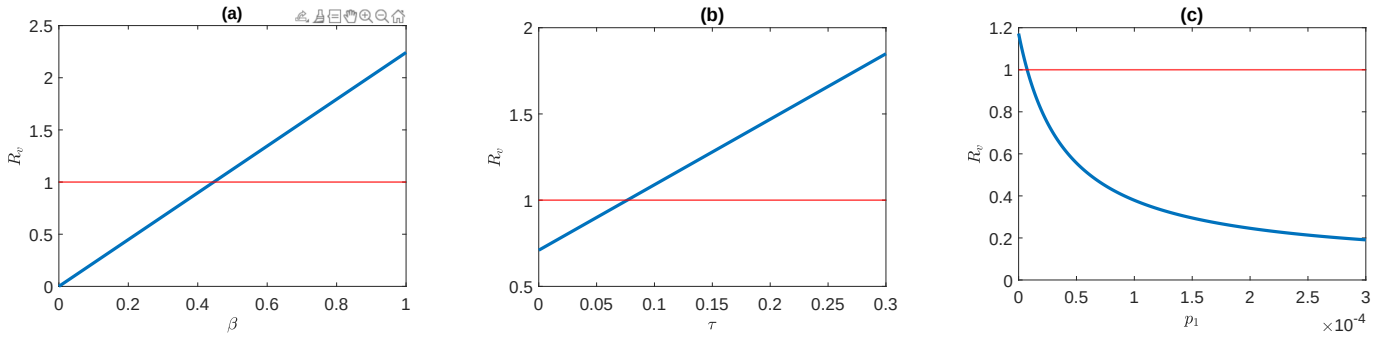

Figure 4: Variation of R_v with respect to : the transmission rate β ,panel (a), to infectivity factor of asymptomatic individuals τ, panel (b) and first dose vaccination rate p_1, panel (c). Other parameter values are given in Table 2.

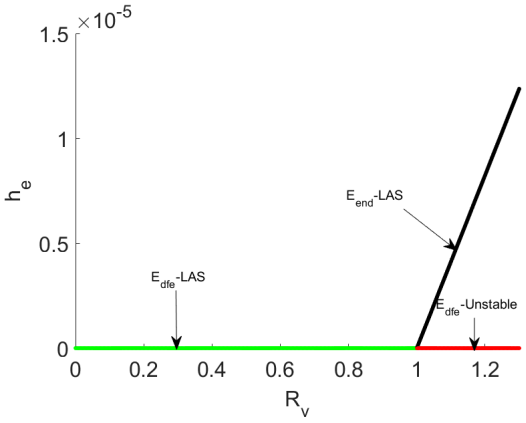

Figure 5: Transcritical bifurcation of model (2) when $R_v = 1$.

4.4 The impact of transmission rate

In this and subsequent subsections, we say infectious population to refer to the sum of the population in symptomatic and asymptomatic classes per time $(I_a(t) + I_s(t))$. This is due to the fact that in our model we assumed people in these two compartments are potential transmitters of the disease. Unless explicitly mentioned, when we say vaccinated individuals, it refers to the total number of individuals vaccinated either with the first dose or the second dose per unit time $(V_1(t)+V_2(t))$. Figure 6 shows the role of the transmission rate β on the dynamics of the infectious, vaccinated, and hospitalized classes. A decrease in the transmission rate results in a prevalence decrease. When the transmission rate is equal to 0.55 $days^{-1}$ the prevalence reaches a high peak of 1424101, but by decreasing it to $\beta = 0.49$ $days^{-1}$ (below the fitted value) the infectious peak can be decreased to 410094 Figure 6 panel (a). This shows that if we can further decrease the transmission rate, it is possible to achieve an infectious number of insignificant value and eradication of the disease. When the transmission rate is small, a small number of people will be infected, which means the number of people in the susceptible class will be large, hence the number of vaccinated people will rise, Figure 6, panel(b). The burden of hospitalization can be decreased by decreasing the transmission rate. As it can be seen in Figure 6, panel(c), when the infectious population is high, correspondingly we have a large number of individuals in the hospital and vice versa.

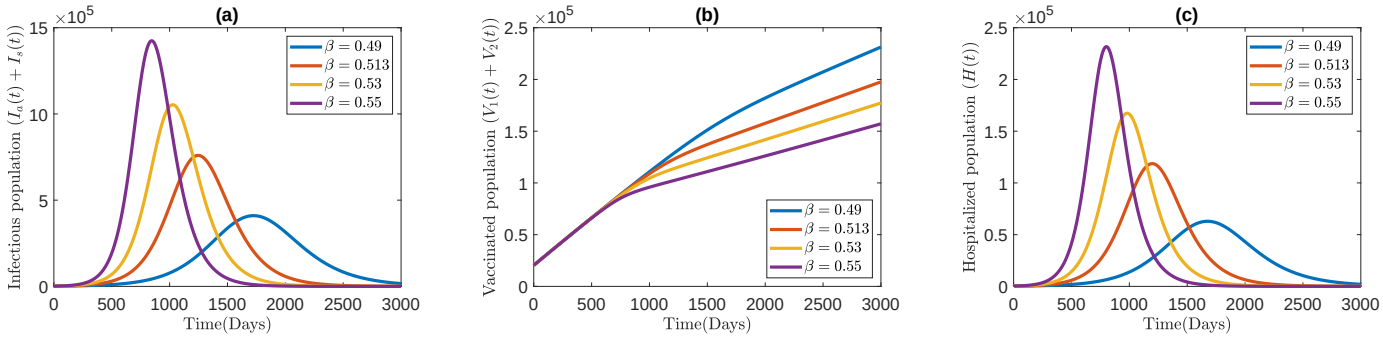

Figure 6: The effect of transmission rate β. Panel (a): infectious population $I_a(t) + I_s(t)$, panel (b): Vaccinated population, $V_1(t) + V_2(t)$, and panel (c) hospitalized individuals. Other parameter values are given in the Table 2.

4.5 The impact of first dose vaccination rate

Figure 7 shows the role of the first dose vaccination rate on the dynamics of infectious, vaccinated and hospitalized population. Increasing this vaccination rate results in a decrease of infectious and hospitalized population Figure 7 panels $(a)\&(c)$. For example when $p_1 = 8.16 \times 10^{-7}\ days^{-1}$ the infectious population reaches a high peak of value 759544 and hospitalized peak of 118624 individuals. If we are able to increase the rate to $p_1 = 8.16 \times 10^{-5}\ days^{-1}$ the above peaks will decrease to 171226 and 26151 of infectious and hospitalized individuals respectively. Such a decrease in prevalence is achieved with high proportion of vaccinated individuals in the population Figure 7 panel (b). Simulation results shows that the role of the second dose vaccination rate, p_2 and time delay between the two doses, α doesn't have significant impact on the dynamics.

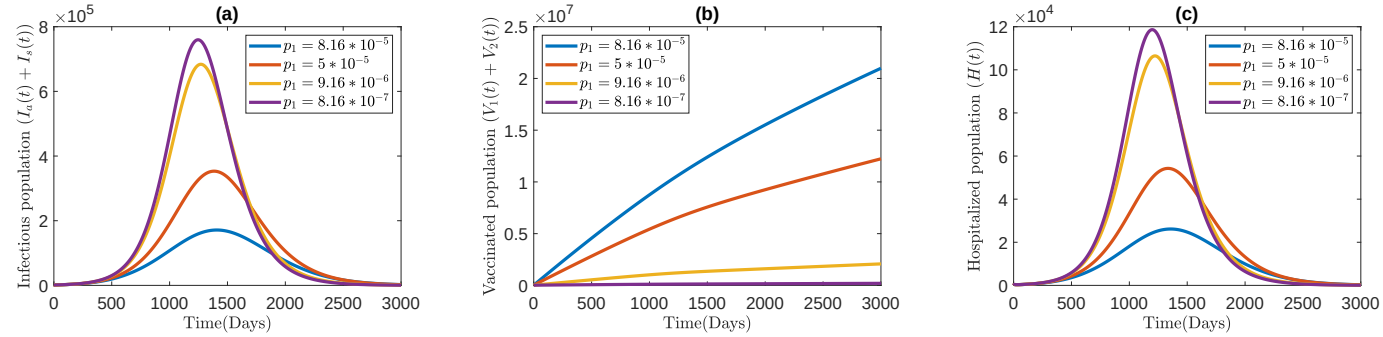

Figure 7: The impact of the first dose vaccination rate p_1: on the dynamics of infectious population,panel (a), vaccinated population, panel (b), and hospitalized population, panel (c). Other parameter values are given in the Table 2.

4.6 The impact of the infectivity factor of asymptomatic individuals

According to the study [22], asymptomatic cases of COVID-19 are a potential source of substantial spread of the disease within the community and one of the results found was people with asymptomatic COVID-19 are infectious but might be less infectious than symptomatic cases. Since the majority of COVID-19 infected individuals become asymptomatic, even if they are less infectious than the symptomatic individuals, their role in spreading the disease may be significant. Figure 8 proves this hypothesis. As the infectivity factor increases, we observed a rise of the infectious population to a relatively high pick (2799983 infectious for $\tau = 0.2$) Figure 8, panel (a), which is not observed in the impact of other parameters, like β. Decreasing the infectivity factor

decreases the infectious population significantly. As observed in other plots here also the increase of infectious population will result in increase in the number of hospitalized individuals and vice versa Figure 8 panel (c). The increase in the infectivity factor τ makes more people to be infected from vaccinated compartments which results in a decrease in the number of vaccinated individuals, Figure 8 panel (b). Therefore the number of vaccinated individuals is inversely proportional to the infectivity factor.

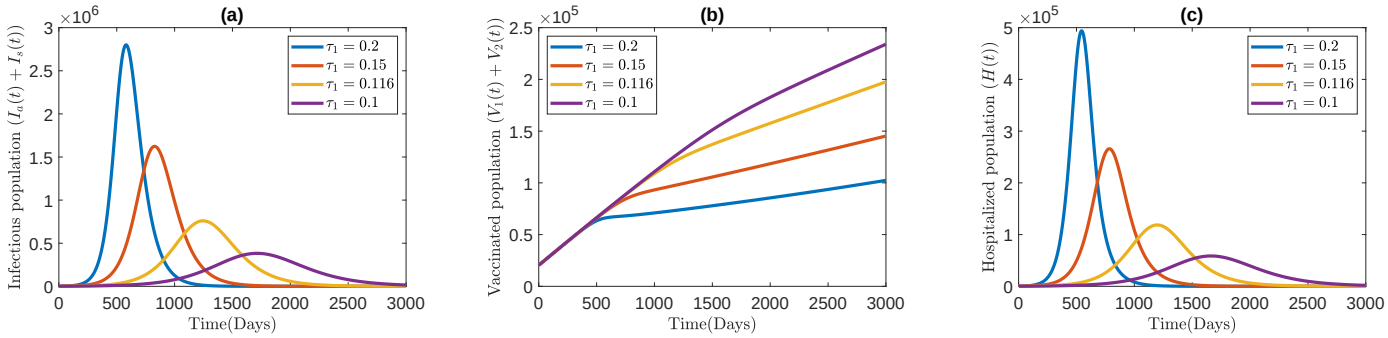

Figure 8: The impact of the infectivity coefficient of asymptomatic population, τ_1 on the dynamics of infectious population,panel (a), total vaccinated population, panel (b), and hospitalized population, panel (c). Other parameter values are as in the Table (2).

5. Prediction of cumulative vaccine dose administered with respect to the first dose vaccination rate.

Most of COVID-19 vaccines approved by WHO are being offered in two doses and a booster. In Ethiopia Sinopharm, AstraZeneca, Johnson and Johnson/Janssen, and Pfizer-BioNTech vaccines are being used. From these vaccines except Johnson&Johnson/Janssen all are being given in two doses. The total number of COVID-19 vaccine dose administered from May 01, 2021 to January 31, 222 (276 days) is 9517539. Using the fitted parameters, our model estimates this number by 9152542 vaccine doses (See, the highlighted row third column of Table 3). If the first dose vaccine administration rate remains the same for the next two years, $(i.e$ after 1006 days) 66483093 number of vaccine doses will be administered. According to World Population Review projection, Ethiopian population in 2024 will be 126.8 million [26]. Since a person can get vaccinated with two doses, we can approximate the number of people vaccinated with at least one dose by $\frac{1}{2} \times$ number of vaccine dose administered. This means 33241546 number of people (Approximately 26% of the total population (in 2024)) will get at least one dose of COVID-19 vaccination. Increasing p_1 to $3.16 \times 10^{-6}\ days^{-1}$ it can be achieved, after two years, 199688874 number of administered vaccine doses. Which is equivalent to 99844437 number of people (approximately 79% of the total population in the year 2024) can get at least first dose (see fourth row of Table 3).

p_1	R_v	Vaccine dose administered in $[0, 276]$ days (Interval of fitting time)	Predicted after two years ($[0, 1006]$ days interval)
$8.157 \times 10^{-7}\ days^{-1}$	1.15	9152542	66483093
$9.16 \times 10^{-7}\ days^{-1}$	1.147	9588497	72169187
$1.16 \times 10^{-6}\ days^{-1}$	1.141	10652193	86042042
$3.16 \times 10^{-6}\ days^{-1}$	1.09	19369216	199688874

Table 3: Values of: Control reproduction number (second column), cumulative vaccine administered at the end of the parameter fitting time (third column) and Predicted number of cumulative vaccine to be administered (fourth column). For different values of p_1. Other parameter values are given in Table 2. The light Cyan shaded row is for the base line p_1 value.

6. Conclusion

In this study, we used a compartmental model for COVID-19 transmission with vaccination. We divided the vaccinated portion of the population into two: Vaccinated with the first dose and fully vaccinated (those who got the two doses). Using the next generation matrix we found a reproduction number which exists when vaccination is in place, we called this parameter as the control reproduction number and denoted it by R_v. We calculated the disease-free and endemic equilibrium of model (2) and showed that the disease-free equilibrium E_{dfe} is globally asymptotically stable if the control reproduction number $R_v < 1$ and unstable if $R_v > 1$. We performed a center manifold analysis based on the method mentioned in Castillo-Chavez and Song[6] and found that the model exhibits a forward bifurcation at $R_v = 1$, which ensures the nonexistence of the endemic equilibrium below the critical value, $R_v = 1$ and the unique endemic equilibrium which exists for $R_v > 1$ is locally asymptotically stable. This implies the disease can be controlled if $R_v < 1$ and it persists in the population if $R_v > 1$. This directs public health policy makers to work on reducing the control reproduction number to less than unity. We performed a sensitivity analysis from which we obtained that the model is sensitive to p_1, p_2, δ with negative sign and β, τ with positive sign. This shows that increasing the vaccination and quarantine rate and decreasing the transmission rate and infectivity factor of asymptomatic individuals will reduce the disease burden.

We performed model fitting to the Ethiopian real COVID-19 data for the period from May $1, 2021$ to January $31, 2022$ to estimate the unknown parameters in the model. In the numerical simulation section, we support our analytical analysis about the stability of the disease-free and endemic equilibrium using the parameter R_v. The result shows for $R_v > 1$ the endemic equilibrium(which exists only for $R_v > 1$) stabilizes through damped oscillation and the disease-free equilibrium is locally asymptotically stable $R_v < 1$, unstable for $R_v > 1$. From the epidemiological perspective, the disease persists in the population with multiple waves if the control reproduction number is greater than unity and it can be eliminated if $R_v < 1$. We also showed the role of some important parameters on the dynamics of the disease so that we got the following points: Reducing the transmission rate and the infectivity factor of asymptomatic individuals will greatly help in reducing the infection burden. Increasing the first dose vaccination rate has a high impact in reducing the infection. Simulation results shows that the second dose vaccination rate has no significant effect on the dynamics of the infectious population.

Moreover, we also predicted the cumulative vaccine dose administered by changing the first dose vaccination rate. In this prediction, if we increase p_1 to a value $3.16 \times 10^{-7}\ days^{-1}$ after two years, the total vaccine dose administered will reach 1996888974, which will cover approximately 79% of the total population. Therefore, from the numerical simulation and analytical analysis, we summarize that it will be essential to reduce the transmission rate, infectivity factor of asymptomatic cases and increase the vaccination rate, quarantine rate to control the disease. As a future work, we will point out that this model can be extended by including additional interventions (for example nonpharmaceutical interventions), by considering the

384 behavioural aspect, and via an optimal control problems.

385 **Data Availability**

386 Data will be available on request.

387 **Conflict of Interest**

388 The Authors declare that they have no conflicts of interest.

389

References

[1] M. A. Acuña-Zegarra, M. Santana-Cibrian, and J. X. Velasco-Hernandez. Modeling behavioral change and covid-19 containment in mexico: A trade-off between lockdown and compliance. *Mathematical biosciences*, 325:108370, 2020.

[2] V. P. Bajiya, S. Bugalia, and J. P. Tripathi. Mathematical modeling of covid-19: impact of non-pharmaceutical interventions in india. *Chaos: An Interdisciplinary Journal of Nonlinear Science*, 30(11):113143, 2020.

[3] Y. Bo, C. Guo, C. Lin, Y. Zeng, H. B. Li, Y. Zhang, M. S. Hossain, J. W. Chan, D. W. Yeung, K. O. Kwok, et al. Effectiveness of non-pharmaceutical interventions on covid-19 transmission in 190 countries from 23 january to 13 april 2020. *International Journal of Infectious Diseases*, 102:247–253, 2021.

[4] B. Buonomo and R. Della Marca. Effects of information-induced behavioural changes during the covid-19 lockdowns: the case of italy. *Royal Society open science*, 7(10):201635, 2020.

[5] B. Buonomo, R. Della Marca, A. d'Onofrio, and M. Groppi. A behavioural modelling approach to assess the impact of covid-19 vaccine hesitancy. *arXiv preprint arXiv:2106.11745*, 2021.

[6] C. Castillo-Chavez and B. Song. Dynamical models of tuberculosis and their applications. *Mathematical Biosciences & Engineering*, 1(2):361, 2004.

[7] C. C. Chavez, Z. Feng, and W. Huang. On the computation of r0 and its role on global stability. *Mathematical Approaches for Emerging and Re-emerging Infection Diseases: An Introduction*, 125:31–65, 2002.

[8] N. Chitnis, J. M. Hyman, and J. M. Cushing. Determining important parameters in the spread of malaria through the sensitivity analysis of a mathematical model. *Bulletin of mathematical biology*, 70(5):1272, 2008.

[9] P. Das, R. K. Upadhyay, A. K. Misra, F. A. Rihan, P. Das, and D. Ghosh. Mathematical model of covid-19 with comorbidity and controlling using non-pharmaceutical interventions and vaccination. *Nonlinear Dynamics*, pages 1–15, 2021.

[10] C. T. Deressa and G. F. Duressa. Modeling and optimal control analysis of transmission dynamics of covid-19: the case of ethiopia. *Alexandria Engineering Journal*, 60(1):719–732, 2021.

[11] O. Diekmann and J. A. P. Heesterbeek. *Mathematical epidemiology of infectious diseases: model building, analysis and interpretation*, volume 5. John Wiley & Sons, 2000.

[12] O. Diekmann, J. A. P. Heesterbeek, and J. A. Metz. On the definition and the computation of the basic reproduction ratio r 0 in models for infectious diseases in heterogeneous populations. *Journal of mathematical biology*, 28(4):365–382, 1990.

[13] S. E. Eikenberry, M. Mancuso, E. Iboi, T. Phan, K. Eikenberry, Y. Kuang, E. Kostelich, and A. B. Gumel. To mask or not to mask: Modeling the potential for face mask use by the general public to curtail the covid-19 pandemic. *Infectious Disease Modelling*, 5:293–308, 2020.

[14] B. A. Ejigu, M. D. Asfaw, L. Cavalerie, T. Abebaw, M. Nanyingi, and M. Baylis. Assessing the impact of non-pharmaceutical interventions (npi) on the dynamics of covid-19: A mathematical modelling study of the case of ethiopia. *PloS one*, 16(11):e0259874, 2021.

[15] Z. S. Kifle and L. L. Obsu. Mathematical modeling for covid-19 transmission dynamics: A case study in ethiopia. *Results in Physics*, page 105191, 2022.

[16] K. G. Mekonen, T. G. Habtemicheal, and S. F. Balcha. Modeling the effect of contaminated objects for the transmission dynamics of covid-19 pandemic with self protection behavior changes. *Results in Applied Mathematics*, 9:100134, 2021.

[17] S. Moore, E. M. Hill, M. J. Tildesley, L. Dyson, and M. J. Keeling. Vaccination and non-pharmaceutical interventions for covid-19: a mathematical modelling study. *The Lancet Infectious Diseases*, 21(6):793–802, 2021.

[18] C. N. Ngonghala, E. Iboi, S. Eikenberry, M. Scotch, C. R. MacIntyre, M. H. Bonds, and A. B. Gumel. Mathematical assessment of the impact of non-pharmaceutical interventions on curtailing the 2019 novel coronavirus. *Mathematical biosciences*, 325:108364, 2020.

[19] Our World in Data. Ethiopia: Coronavirus pandemic country profile. `https://ourworldindata.org/coronavirus/country/ethiopia`, 2021. (Accessed on Feb 05, 2022).

[20] T. A. Perkins and G. España. Optimal control of the covid-19 pandemic with non-pharmaceutical interventions. *Bulletin of Mathematical Biology*, 82(9):1–24, 2020.

[21] H. Ritchie, E. Mathieu, L. Rodés-Guirao, C. Appel, C. Giattino, E. Ortiz-Ospina, J. H. B. Macdonald, D. Beltekian, and M. Roser. Coronavirus pandemic (covid-19). *Our World in Data*, 2021. https://ourworldindata.org/covid-vaccinations.

[22] A. A. Sayampanathan, C. S. Heng, P. H. Pin, J. Pang, T. Y. Leong, and V. J. Lee. Infectivity of asymptomatic versus symptomatic covid-19. *The Lancet*, 397(10269):93–94, 2021.

[23] A. Ssematimba, J. Nakakawa, J. Ssebuliba, and J. Y. Mugisha. Mathematical model for covid-19 management in crowded settlements and high-activity areas. *International Journal of Dynamics and Control*, pages 1–12, 2021.

[24] WHO. 10 vaccines granted emergency use listing (eul) by who. `https://covid19.trackvaccines.org/agency/who/`, 2022. (Accessed on March 09, 2022).

[25] WHO. Who coronavirus (covid-19) dashboard. `https://covid19.who.int/`, 2022. (Accessed on March 09, 2022).

[26] World Population Review. Ethiopia population projections. `https://worldpopulationreview.com/countries/ethiopia-population`, 2022. (Accessed on March 08, 2022).

[27] Worldometer. Ethiopia demographics. `https://www.worldometers.info/demographics/ethiopia-demographics/`, 2021. (Accessed on Feb 05, 2022).